Deterministic lattice Lorentz gas. II. Mirror model

1991 J. Phys. A: Math. Gen. 24 807

(http://iopscience.iop.org/0305-4470/24/4/015)

J. Phys. A: Math. Gen. 24 (1991) 807–825. Printed in the UK

Deterministic lattice Lorentz gas: II. Mirror model

G A van Velzen

Institute for Theoretical Physics, Princetonplein 5, PO Box 80006, 3508 TA Utrecht, The Netherlands

Received 31 July 1990

Abstract. As a model for diffusion, a lattice version of the Lorentz gas is studied, using specular collision rules. A previously developed theory, containing the molecular chaos approximation, several ring approximations and the effective medium approximation (EMA), is applied and compared with simulations. The correction to the Boltzmann equation result, resulting from effective medium approximation (EMA) is opposite to the simulation results. This indicates that other diagrams than ring diagrams should be considered, which is peculiar if one considers the successes of the EMA for other models. This is investigated by using variants of the model. The diffusion tensor is in general non-isotropic; the corresponding features are qualitatively described by theory.

1. Introduction

In the widely studied class of models known as cellular automata (CA) [1–6], a subclass consists of lattice versions of the Lorentz gas. The classical Lorentz gas has been used extensively for studying diffusion [7–14]. The model is defined by a random *static* array of scatterers, in which independent particles move ballistically in between two collisions with scatterers. The scatterers may have different shapes, such as hard spheres, pins, diamond shapes, squares etc, and the collisions are usually elastic. The *lattice* version has scatterers that reside on the sites of a lattice, in a random but fixed configuration. The analogue of different shapes of the scatterers are here the different collision rules that can be chosen to describe the interaction of the moving particles with the scatterers. In previous papers we have used probabilities to describe the outcome of the collisions [15–18]. However, it may be preferable to consider deterministic (reversible) laws to describe the microscopic dynamics. In order to do so, we discussed the *chiral model* [19], for which we refer to the preceding paper [20]. In this model a scatterer rotates the direction of the velocity of the incoming particle over an angle that depends on the type of the scatterer. The theory that we developed to describe the model with stochastic collision rules was generalized successfully to the chiral model. However, some effects that seem to arise from the deterministic character result in differences between theory and computer simulations for the chiral model.

Therefore we want to study a different choice of the collision rules, in order to gain more insight into the dependence of the results on the specific choice of the deterministic collision rules.

In this paper we will apply the theory to the mirror model of Ruijgrok and Cohen [22]. This model is known to show peculiar behaviour, as results from extensive

0305-4470/91/040807+19$03.50

computer simulations indicate [23–25]. The behaviour is rather different from what one would expect from one's knowledge of the stochastic model of [17] or the chiral model of [20]. Because of the deterministic collision rules, the path of an individual ballistically moving particle is completely determined once the scatterer configuration, the starting position of the particle and its initial velocity are known. The model is defined in two dimensions, but one may consider higher-dimensional generalizations, as we will mention later.

The outcome of a collision of a moving particle with a scatterer is completely determined by the direction of the incident particle and the type of scatterer. As in the chiral model, the direction is turned over 90°, but there is an essential difference in the way this depends on the scatterer type: the scattering rules are such that we can think of the scatterers as mirrors that are placed at random on the lattice sites. The orientation of the mirrors makes a 45° angle with the lattice axes. There are two types of mirrors (see figure 1), and originally the model did not contain reflectors [22]. For the subsequent analysis it is, however, straightforward to include reflections. For reasons of completeness it is even necessary to do so: our self-consistent calculations will in general generate a matrix of effective transition rates that has a non-zero entry for the reflection probability.

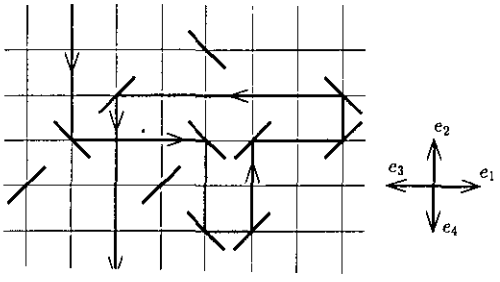

Figure 1. Mirror model.

The particles may be (will be) trapped in closed orbits, of which the length distribution has been investigated [22]. For an illustration we refer to figure 1, where we show an example of a particle trajectory. A justification for omitting reflectors in actual simulations is that the moving particle will retrace its path *completely* once a reflector is hit; a pathological one-dimensional feature that one may wish to avoid.

As the scattering direction is 'attached' to the lattice, anisotropy will be observed if the densities of left- and right-oriented mirrors are unequal, and in general the elements of the diagonalized diffusion tensor are not equal (see later).

A generalization to three dimensions can be constructed in a straightforward manner [26].

For the two-dimensional model, extensive computer simulations have been carried out. The majority of them concern the diffusion coefficient, defined as the long-time limit of the time-dependent diffusion coefficient $D(t) \equiv \frac{1}{2}\partial_t\langle x^2\rangle$, i.e. one basically looks at the second moment of the distribution of the moving particles. Although early simulations could still be explained by the Boltzmann approximation [22], later simulations with higher statistics definitely demonstrated a *positive* deviation from Boltzmann [23–25]. This is remarkable, because in Lorentz gases of the standard type, like the continuous Lorentz gases [12, 13], hopping models [27–32], and the stochastic

lattice Lorentz gas of [17], one usually finds *negative* corrections to Boltzmann. These come from ring collisions, giving rise to negative contributions to the VACF.

In contrast with Lorentz gases, *fluids* have ring integrals that lead to *positive* velocity correlations (phenomenologically interpreted in terms of vortex flow), and the experimental and simulation results for the diffusion coefficient are always larger than what the Boltzmann approximation predicts.

For the present model with equal numbers of right and left mirrors, Kong and Cohen [23] were able to explain the sign, but not the magnitude of this deviation by an intuitive argument in terms of local fluctuations of excesses of right mirrors or of left mirrors. A similar effect was studied in the 'pipeline'-like trajectories between two nearby 'trees' in the Ehrenfest wind-tree model [33]. Both types of fluctuations lead to an increase of the diffusion coefficient. Unfortunately it is not obvious how to relate these fluctuations to any special sequence of correlated collisions [17, 18], and how to incorporate them in a kinetic theory analysis. Therefore it is worthwhile to investigate the mirror model with the help of our approximate kinetic equations. In order to investigate the origin of the deviations, we also performed simulations with transmitting and flipping mirrors.

A variant of the mirror model (also studied in [22] and [23]) is one in which the mirrors flip orientation upon being hit by a moving particle. In the case that we have more than one moving particle in the system (diffusion is usually pictured in terms of the spreading of a cloud of particles), this clearly introduces interactions between the moving particles and strictly speaking the model cannot be considered as a Lorentz gas of non-interacting moving particles. However, if one considers only one moving particle the model does have the characteristics of a Lorentz gas. In addition, the distribution function of the left and right mirrors tends to a fifty–fifty distribution, due to collisions with the moving particle. Computer simulations show that the diffusion coefficient, in the case that there is only one particle present in the system, surprisingly coincides with the results for more moving particles [23]. The interaction with the flipping mirrors mainly randomizes the scatterings, and thus increases the validity of kinetic theory arguments. We will consider variants of the mirror model to investigate this further.

We mention some other properties of the model. An interesting feature is that the probability distribution of displacements is non-Gaussian, which is reflected in the fourth moment of the probability distribution [23]. Therefore the probability distribution of displacements does not satisfy a diffusion equation. Finally, the full lattice with equal amounts of the two types of mirrors ($\gamma^{\mathrm{L}} = \gamma^{\mathrm{R}} = \frac{1}{2}$) can be mapped onto the bond percolation model at criticality, and the critical exponents of the moments can be calculated [34, 23].

Before starting the analysis in the next sections, we introduce some notation. A lattice site is either empty (with probability $\alpha = 1 - c$), or contains one of the three types of scatterers: left-mirrors (with probability γ^{L}), right-mirrors (with probability γ^{R}) or reflectors (with probability β). The probabilities are normalized by

$$\alpha + \beta + \gamma^{\mathrm{L}} + \gamma^{\mathrm{R}} = 1. \tag{1.1}$$

By introducing the concentration $c = 1 - \alpha$ of occupied sites, we have also

$$\beta + \gamma^{\mathrm{L}} + \gamma^{\mathrm{R}} = c. \tag{1.2}$$

We can write down the generalization of the theory of [17, 18], derived in detail in [20]. Where necessary we will repeat the formulae we need, without giving the

detailed explanation. We will give the Chapman–Kolmogorov equation for this model (section 2) and consider the symmetry group of the collision operators (section 3). The Boltzmann approximation (section 4), the ring and repeated-ring approximations and their corresponding self-consistent versions (section 5) and the full effective medium approximation (EMA, section 6) will be analysed. We will discuss flipping and transmission in section 7. The results will be compared with computer simulations. We will also consider a case that has a non-isotropic diffusion tensor.

2. Chapman–Kolmogorov equation

We will discuss the two-dimensional version of the mirror model. The equation of motion is the Chapman–Kolmogorov (CK) equation, which can be written down after assigning to every lattice site n the stochastic variables α_n, β_n, γ_n^{L} and γ_n^{R}. Each of them can take on the values 0 or 1, subject to the constraint $\alpha_n + \beta_n + \gamma_n^{\mathrm{L}} + \gamma_n^{\mathrm{R}} = 1$: for given n only one of them is different from zero. The CK equation is then given by [17,35]

$$p(n + e_i, i, t+1) = \alpha_n p(n,i,t) + \beta_n \sum_j W_{ij}^{\mathrm{B}} p(n,j,t)$$
$$\gamma_n^{\mathrm{L}} \sum_j W_{ij}^{\mathrm{L}} p(n,j,t) + \gamma_n^{\mathrm{R}} \sum_j W_{ij}^{\mathrm{R}} p(n,j,t) \tag{2.1}$$

where the transition matrices for the velocities, defined on the basis $\{e_1, e_2, e_3, e_4\}$ of figure 1, are

$$W^A = 1 = \begin{pmatrix} 1 & 0 & 0 & 0 \\ 0 & 1 & 0 & 0 \\ 0 & 0 & 1 & 0 \\ 0 & 0 & 0 & 1 \end{pmatrix} \qquad W^{\mathrm{B}} = \begin{pmatrix} 0 & 0 & 1 & 0 \\ 0 & 0 & 0 & 1 \\ 1 & 0 & 0 & 0 \\ 0 & 1 & 0 & 0 \end{pmatrix}$$
$$W^{\mathrm{L}} = \begin{pmatrix} 0 & 0 & 0 & 1 \\ 0 & 0 & 1 & 0 \\ 0 & 1 & 0 & 0 \\ 1 & 0 & 0 & 0 \end{pmatrix} \qquad W^{\mathrm{R}} = \begin{pmatrix} 0 & 1 & 0 & 0 \\ 1 & 0 & 0 & 0 \\ 0 & 0 & 0 & 1 \\ 0 & 0 & 1 & 0 \end{pmatrix}. \tag{2.2}$$

One easily verifies that $(W^{\mathrm{L}})^2 = (W^{\mathrm{R}})^2 = 1$ and that $W^{\mathrm{L}}W^{\mathrm{R}} = W^{\mathrm{R}}W^{\mathrm{L}} = W^{\mathrm{B}}$. As mentioned before, the matrix that describes reflection (W^{B}) is included here for reasons of completeness. As in [20], (2.1) can formally be written in 4-vector and $4N$-matrix notation:

$$p(t+1) = S^{-1}(1+K)p(t) \tag{2.3}$$

where S is the free streaming operator and K the collision operator, see [20].

$$K_n = \beta_n T^{\mathrm{B}} + \gamma_n^{\mathrm{L}} T^{\mathrm{L}} + \gamma_n^{\mathrm{R}} T^{\mathrm{R}} \tag{2.4}$$

where $T^X \equiv W^X - 1$, with the W defined in (2.2).

3. Symmetries

For later convenience, we again diagonalize the operators in velocity space [17,20]. For the present model, it turns out that we have to define a basis in velocity space, that is different from those used in [17] and [20]. The choice of the basis is related to the symmetry of the transition matrices. Using the matrices given in (2.2), which form a basis, any general reflection-symmetric matrix can be written as

$$H = a1 + bW^{\mathrm{B}} + c^{\mathrm{L}}W^{\mathrm{L}} + c^{\mathrm{R}}W^{\mathrm{R}}. \tag{3.1}$$

We use a vector notation for the velocities, where $|V_x\rangle$ and $|V_y\rangle$ are column vectors with components $(1,0,-1,0)$ and $(0,1,0,-1)$, respectively, on the basis e_1, e_2, e_3, e_4, defined in figure 1. Together with $|1\rangle = (1,1,1,1)$ and $|2V_x^2 - 1\rangle = (1,-1,1,-1)$ they represent a basis of the four-dimensional velocity space in the case that we have the full cubic symmetry (see [17] for more details). One can easily verify that $|V_x\rangle$ and $|V_y\rangle$, which are eigenvectors of the matrices with the full cubic symmetry [17], do not serve as such for the matrices given in (3.1). But, using the commutativity of the matrices given in (2.2), we can diagonalize the general reflection symmetric matrix H. One can verify that this is realized by replacing the set $\{|V_x\rangle, |V_y\rangle\}$ by the set $\{|V_+\rangle, |V_-\rangle\}$ in the following way:

$$|V_+\rangle = |V_x\rangle + |V_y\rangle \qquad |V_+\rangle = |V_x\rangle - |V_y\rangle. \tag{3.2}$$

This transformation essentially diagonalizes the anisotropy of the model. Next we introduce eigenvectors

$$|\psi_o\rangle = |1\rangle \qquad |\psi_1\rangle = |V_+\rangle \qquad |\psi_2\rangle = |V_-\rangle \qquad |\psi_3\rangle = |V_x^2 - V_y^2\rangle \tag{3.3}$$

which are normalized with respect to the (real) inner product

$$\langle a(V)|b(V)\rangle \equiv \frac{1}{4}\sum_i a(e_i)b(e_i). \tag{3.4}$$

The eigenvalues of (3.1) corresponding to (3.3) are:

$$\begin{aligned} h_0 &= a + b + c^{\mathrm{L}} + c^{\mathrm{R}} \\ h_1 &= h_+ = a - b - c^{\mathrm{L}} + c^{\mathrm{R}} \\ h_2 &= h_- = a - b + c^{\mathrm{L}} - c^{\mathrm{R}} \\ h_3 &= a + b - c^{\mathrm{L}} - c^{\mathrm{R}}. \end{aligned} \tag{3.5}$$

Using this, the collision operators, $T^X \equiv W^X - 1$, are seen to have the following eigenvalues, see (2.2):

$$\begin{array}{lll} t_1^{\mathrm{B}} = -2 & t_1^{\mathrm{L}} = -2 & t_1^{\mathrm{R}} = 0 \\ t_2^{\mathrm{B}} = -2 & t_2^{\mathrm{L}} = 0 & t_2^{\mathrm{R}} = -2 \\ t_3^{\mathrm{B}} = \ \ 0 & t_3^{\mathrm{L}} = -2 & t_3^{\mathrm{R}} = -2. \end{array} \tag{3.6}$$

The generalization of the Green–Kubo expression for the 'total' diffusion coefficient to the present model is the same as we found in the preceding paper for the chiral model, i.e.

$$D = \frac{1}{4}\sum_{\ell=1}^{2}\langle\psi_\ell|\hat{\Gamma}(q=0,z=0)|\psi_\ell\rangle - \tfrac{1}{4} = \tfrac{1}{4}\left(\lambda_+^{-1} + \lambda_-^{-1} - 1\right) \tag{3.7}$$

with the vector eigenvalues $\lambda_+^{-1}(=\lambda_1^{-1})$ and $\lambda_-^{-1}(=\lambda_2^{-1})$ of the operator $\langle\hat{\Gamma}(0,0)\rangle$. $\hat{\Gamma}(q,z)$ is the Fourier–Laplace transformed propagator $[(1+z)S - 1 - K]^{-1}$; see [17,18,20] for details. However, for this model we can introduce 'partial' diffusion coefficients, that are defined on the basis that diagonalizes the problem: instead of taking the diffusion coefficient to be the time derivative of the mean square displacement $\langle n_x^2 + n_y^2\rangle$, we define the partial coefficients as time derivatives of $\langle(n_x + n_y)^2\rangle$ and $\langle(n_x - n_y)^2\rangle$, respectively. This is worked out in detail in appendix 1. The result is two partial diffusion coefficients D_+ and D_-:

$$D_\pm = \frac{1}{2\lambda_\pm} - \frac{1}{4}. \tag{3.8}$$

The total coefficient is then given by $D = \frac{1}{2}(D_+ + D_-)$, equivalent to (3.7). The analogue for the chiral model would be a separation in two opposite 'chiral' terms of the diffusion coefficient. These quantities cannot be visualized straightforwardly, while D_+ and D_- for the mirror model can easily be measured in a simulation.

In the subsequent sections we will discuss various approximation schemes to obtain the eigenvalues λ_+ and λ_-.

4. Boltzmann approximation

In the Boltzmann approximation one neglects correlations between collisions, and the configuration average reduces to a single-site average. The Boltzmann collision operator is then

$$K^0 = \langle K\rangle = \beta T^{\mathrm{B}} + \gamma^{\mathrm{L}} T^{\mathrm{L}} + \gamma^{\mathrm{R}} T^{\mathrm{R}} \tag{4.1}$$

For the 'total' diffusion coefficient (3.7) we need the eigenvalues λ_+ and λ_- of this operator, i.e.

$$\begin{aligned} \lambda_+ &= -\beta t_1^{\mathrm{B}} - \gamma^{\mathrm{L}} t_1^{\mathrm{L}} - \gamma^{\mathrm{R}} t_1^{\mathrm{R}} = 2\beta + 2\gamma^{\mathrm{L}} \\ \lambda_- &= -\beta t_2^{\mathrm{B}} - \gamma^{\mathrm{L}} t_2^{\mathrm{L}} - \gamma^{\mathrm{R}} t_2^{\mathrm{R}} = 2\beta + 2\gamma^{\mathrm{R}} \end{aligned} \tag{4.2}$$

(see (3.6)). We see that for the usual mirror model ($\beta = 0$) the λ_+ and λ_- term are just given by the densities of left- and right-oriented mirrors, respectively. For either type of mirror, the reflection is in the $(1,\pm1)$ direction, which is just the basis vector corresponding to the $\pm$ direction that came out of the diagonalization procedure. Neglecting correlations between collisions (which is done by taking the Boltzmann approximation) thus immediately decouples the two contributions to the diffusion coefficient. In the case that we have only one type of mirror (say right-mirrors, see

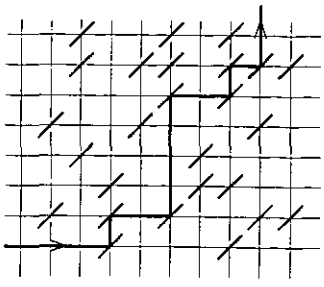

Figure 2. Exactly solvable model.

figure 2), the λ_+-part of the diffusion coefficient diverges. This corresponds to straight-line motion in a diagonal direction. The λ_- component is then *exactly* given by the Boltzmann result, because returns are impossible and all collisions are uncorrelated, making the Boltzmann approximation exact.

In the Boltzmann approximation the diffusion coefficient $D = \frac{1}{2}(D_+ + D_-)$ is in general given by

$$D^0 = \frac{1}{8}\,\frac{2\beta + \gamma^{\mathrm{L}} + \gamma^{\mathrm{R}}}{\beta^2 + \beta(\gamma^{\mathrm{L}} + \gamma^{\mathrm{R}}) + \gamma^{\mathrm{L}}\gamma^{\mathrm{R}}} - \frac{1}{4}. \tag{4.3}$$

For the case $\beta = 0$, $\gamma^{\mathrm{R}} = \gamma^{\mathrm{L}} = \frac{1}{2}c$ this yields $D = \frac{1}{2}c - \frac{1}{4}$ [22].

5. Ring and repeated-ring approximation

We note the following properties of deterministic lattice Lorentz gases models. In the mirror model (without reflections) a particle can never retrace part of its trajectory in the opposite direction, as opposed to the chiral model. Therefore a particle can return at most *twice* to the same site before being trapped in a periodic orbit, whereas in the chiral model this can happen four times [19]. We recall from [17, 18] that for the stochastic model no periodic orbits exist, and the trajectory between subsequent repeated returns more likely consists of uncorrelated collision sequences. This makes the dynamics summed by the RRA and the EMA more appropriate for the continuous Lorentz gas, hopping models and the ballistic lattice Lorentz gas with stochastic collision rules, than for the deterministic lattice models.

The formulation of the ring and repeated-ring approximations (RA and RRA) and their self-consistent counterparts for the mirror model is analogous to what we have done for the chiral model of [20], the preceding paper, so we do not have to repeat the formalism here.

For the mirror model we do not have an exact solution for the completely filled lattice. As the ring integral depends both on the λ_+ and the λ_- eigenvalue, the ring and repeated-ring approximations already destroy the decoupling of the + and − contributions that occurs in the Boltzmann approximation.

The approximations discussed before are obtained by making specific choices for the $\lambda_\ell = -k_\ell^0 - b_\ell$, where the k_ℓ^0 are the eigenvalues of the Boltzmann collision operator (4.1), and b_ℓ are those for the collision diagrams, explicitly given in operator expressions in the preceding paper [20].

6. Effective medium approximation

The effective medium approximation, which has been applied successfully to random resistor networks, hopping models and the stochastic lattice Lorentz gas [17,18,32,36,37], has been generalized to a model with more types of different scatterers in [20]. Most of the formalism developed there, can be copied for the mirror model. In general the effective medium condition

$$\left\langle \frac{K_n - cT^{\mathrm{e}}}{1 - R(K_n - cT^{\mathrm{e}})} \right\rangle = 0 \tag{6.1}$$

yields a fourth-order equation if we consider the eigenvalues of the different operators that occur in the equation, see section 3. However, we will see that, for the specific form of the eigenvectors, the EMA equation will now be two orders lower, as will be explained later. So we have quadratic equations for the effective collision operator eigenvalues λ. The λ are real.

For the mirror model the EMA is determined by the coupled equations for the ring integral (A2.9) and the eigenvalue version of the EMA-condition (6.1). The latter yields the eigenvalues λ_ℓ of $\Lambda = -cT^{\mathrm{e}}$, that can be substituted in (A2.9), through (A2.10) and (A2.11), to calculate the corresponding eigenvalues of the ring operator. For the evaluation of the ring integral we refer to appendix 2, here we first discuss the EMA condition.

First, we have a closer look at the eigenvalues of the collision operators. In terms of the eigenvalues for the mirror model, the EMA equation (6.1) is written explicitly as

$$\alpha \frac{-ct_1^{\mathrm{e}}}{1 - r_1(-ct_1^{\mathrm{e}})} + \beta \frac{-2 - ct_1^{\mathrm{e}}}{1 - r_1(-2 - ct_1^{\mathrm{e}})} + \gamma^{\mathrm{L}} \frac{-2 - ct_1^{\mathrm{e}}}{1 - r_1(-2 - ct_1^{\mathrm{e}})} + \gamma^{\mathrm{R}} \frac{-ct_1^{\mathrm{e}}}{1 - r_1(-ct_1^{\mathrm{e}})} = 0$$

for $\ell = 1$

$$\alpha \frac{-ct_2^{\mathrm{e}}}{1 - r_2(-ct_2^{\mathrm{e}})} + \beta \frac{-2 - ct_2^{\mathrm{e}}}{1 - r_2(-2 - ct_2^{\mathrm{e}})} + \gamma^{\mathrm{L}} \frac{-ct_2^{\mathrm{e}}}{1 - r_2(-ct_2^{\mathrm{e}})} + \gamma^{\mathrm{R}} \frac{-2 - ct_2^{\mathrm{e}}}{1 - r_2(-2 - ct_2^{\mathrm{e}})} = 0 \tag{6.2}$$

for $\ell = 2$, and

$$\alpha \frac{-ct_3^{\mathrm{e}}}{1 - r_3(-ct_3^{\mathrm{e}})} + \beta \frac{-ct_3^{\mathrm{e}}}{1 - r_3(-ct_3^{\mathrm{e}})} + \gamma^{\mathrm{L}} \frac{-2 - ct_3^{\mathrm{e}}}{1 - r_3(-2 - ct_3^{\mathrm{e}})} + \gamma^{\mathrm{R}} \frac{-2 - ct_3^{\mathrm{e}}}{1 - r_3(-2 - ct_3^{\mathrm{e}})} = 0$$

for $\ell = 3$. Here we substituted in the EMA equation the explicit eigenvalues of the collision operators T^X given in (3.6). We see that the denominators always come in pairs. This lowers the order of the equations by two. This simplification does not occur for the chiral model of [20].

The diffusion coefficient is given by (3.7) with the present eigenvalues $\lambda_+ = -ct_1^{\mathrm{e}}$, $\lambda_- = -ct_2^{\mathrm{e}}$, or written as the average of D_+ and D_-, given in (3.8).

From the resulting eigenvalues t_ℓ^{e} of T^{e} in any of the approximations one can calculate effective densities for the different types of scatterers. The matrix equation

$$cT^{\mathrm{e}} = \beta^{\mathrm{e}} T^{\mathrm{B}} + \gamma^{\mathrm{L}^{\mathrm{e}}} T^{\mathrm{L}} + \gamma^{\mathrm{R}^{\mathrm{e}}} T^{\mathrm{R}} \tag{6.3}$$

yields

$$\begin{aligned} \beta^{\mathrm{e}} &= -\tfrac{1}{4} c\,(t_1^{\mathrm{e}} + t_2^{\mathrm{e}} - t_3^{\mathrm{e}}) \\ \gamma^{\mathrm{L}^{\mathrm{e}}} &= \tfrac{1}{4} c\,(-t_1^{\mathrm{e}} + t_2^{\mathrm{e}} - t_3^{\mathrm{e}}) \\ \gamma^{\mathrm{R}^{\mathrm{e}}} &= \tfrac{1}{4} c\,(t_1^{\mathrm{e}} - t_2^{\mathrm{e}} - t_3^{\mathrm{e}}). \end{aligned} \tag{6.4}$$

7. Other mirror models

Here we add to the mirror model the possibility of flipping and transmission. This is interesting for studying the influence of stochastic effects and effects that relate to interaction between the moving particles. We will restrict ourselves to the models that do not have reflectors, i.e. $\beta = 0$. First we study the model in which flipping of the mirror occurs with probability one every time it suffers a collision with a particle. This results in interactions between the moving particles, while the theory we have presented so far concerns essentially only a *single moving particle*. We can modify the theory to deal with the latter. The collision sequences contain alternatingly right- and left-oriented mirrors; in between, the moving particles perform rings. These sequences can be summed, yielding the repeated-ring approximation, for which the collision diagrams are written as

$$B^{\rm fl}_{\rm RRA} = \gamma^{\rm L}\left[T^{\rm R}R^0T^{\rm L} + T^{\rm L}R^0T^{\rm R}R^0T^{\rm L}\right]\left(1 - R^0T^{\rm R}R^0T^{\rm L}\right)^{-1} + \gamma^{\rm R}\left[T^{\rm L}R^0T^{\rm R} + T^{\rm R}R^0T^{\rm L}R^0T^{\rm R}\right]\left(1 - R^0T^{\rm L}R^0T^{\rm R}\right)^{-1}. \tag{7.1}$$

Here we have used R^0, the ring integral over the Boltzmann propagator. We have left out reflectors, but in principle $\gamma^{\rm R}$ and $\gamma^{\rm L}$ do not have to be the same. We work this out using the explicit eigenvalues of the collision operators $T^{\rm L}$ and $T^{\rm R}$, given in (3.6). The result is that for $\ell = 1$ and $\ell = 2$ we have $B^{\rm fl}_{\rm RRA} = 0$, and consequently the diffusion coefficient in RRA coincides with the Boltzmann value. The tensor ($\ell = 3$) eigenvalue is different, and involves the eigenvalue of the ring operator, so it may play a role in a self-consistent scheme. The most important self-consistent approximation scheme is the EMA equation, which we can write down for the flipping mirror model with one moving particle. Instead of repeated visits to alternatingly left- and right-mirrors, we visit repeatedly fluctuations $\delta T^{\rm L} \equiv T^{\rm L} - cT^{\rm e}$ and $\delta T^{\rm R} \equiv T^{\rm R} - cT^{\rm e}$. In fact one splits up the repeated series of the usual EMA into an even and an odd subseries, and makes the two series alternating. Then the EMA equation for the flipping mirror model is

$$\alpha(-cT^{\rm e})(1 - R(-cT^{\rm e}))^{-1} + \gamma^{\rm L}[\delta T^{\rm R}R\delta T^{\rm L} + \delta T^{\rm L}R\delta T^{\rm R}R\delta T^{\rm L}](1 - R\delta T^{\rm R}R\delta T^{\rm L})^{-1} + \gamma^{\rm R}[\delta T^{\rm L}R\delta T^{\rm R} + \delta T^{\rm R}R\delta T^{\rm L}R\delta T^{\rm R}](1 - R\delta T^{\rm L}R\delta T^{\rm R})^{-1} = 0. \tag{7.2}$$

Here, R is the self-consistent ring integral. The result of this exercise is that, also in the context of the full EMA for the flipping mirror model, the diffusion coefficient coincides with the Boltzmann result. Investigation of this with the explicit eigenvalues (3.6) shows that this does not follow from the EMA equation itself: the iteration with the ring integral is needed to obtain this numerical result. This indicates cancellations of diagrams, similar to what we obtained for the stochastic lattice Lorentz gas with only left–right collisions, see [17]. We conclude that accounting for ring and nested-ring type of events does not yield deviations from Boltzmann.

Another model is one in which the mirrors flip orientation only with a certain probability, say $p_{\rm fl}$. With some algebra we can find expressions analogous to (7.1) and (7.2). For this model, simulations (see section 8) show that already for *small* non-zero flip probabilities the diffusion coefficient differs substantially from the fixed-mirror value [21]. The former is smaller and the latter is larger than the Boltzmann value,

as we discuss in section 8. Before commenting on this, we also introduce the mirror model with *transmission* probability $p_{\rm tr}$.

Both introduction of flipping and transmission are intuitively expected to yield better agreement with Boltzmann, as their stochastic properties have a randomizing effect. For *small* values of $p_{\rm fl}$ and $p_{\rm tr}$, however, we observe that the deviations from Boltzmann do not decrease, but merely change sign. Some typical trajectories that may be involved are shown in figure 3. They are orbiting trajectories. We have only drawn the mirrors that we focus on; the actual form of the remaining parts of the trajectories is not relevant. First we discuss the case with a small transmission probability. For the trajectories of figure 3(a) with fixed mirrors, there are positive correlations inside each orbit at either side of the mirror. As a particle leaks through the mirror, which for low $p_{\rm tr}$ is assumed to occur only once on the timescale we consider, it will not return to previously visited sites, and the correlations are lost. However, the trajectory in figure 3(b) hits both sides of the mirror. If the particle leaks through here, it will travel on the same trajectory in the *opposite* direction, and the contributions from correlations get a *negative* sign. Further, in figure 3(c) we have drawn a more complicated orbiting trajectory, for which leaking through only means that the particle 'skips' a part of its trajectory: the sign of the correlation remains positive.

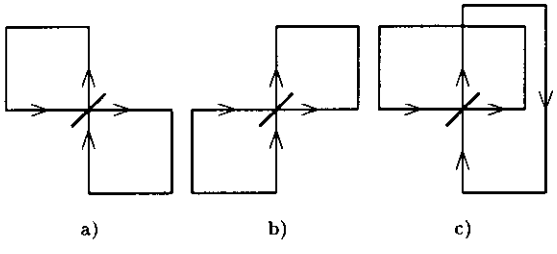

Figure 3. Typical orbiting trajectories.

Similar arguments apply for the case of flipping probability $p_{\rm fl}$, where the mirror is assumed to flip only once. In figure 3(a), the two orbits will be combined to a longer orbit. In figure 3(b) flipping of the mirror will split up the trajectory. Both will occur at the cost of positive correlation. In the trajectory of figure 3(c), however, flipping of the mirror will send the particle in the *opposite* direction, and thus the sign of the correlation contributions from these orbits is changed. As the trajectories of figure 3(c) are more complicated, their effect will be less than in the case of a small transmission probability. For further remarks we refer the reader to section 8.

8. Results and discussion

We calculate the diffusion coefficient for the mirror model using several approximation schemes. Some of them are standardly used in kinetic theory; in addition, we also consider the effective medium approximation (EMA). We choose some typical sets of parameters where, in the spirit of the original model, we usually take $\beta = 0$. Later on, we will briefly report on cases with $\beta \neq 0$. For the present model, the EMA equations (6.2) are only quadratic, in spite of the four terms in occurring in the general EMA

equation (6.1). The ring integral, however, has in general the complicated form (A2.9). We have computed it numerically.

Nevertheless, there exists a subclass of models for which the ring integral does have the same form as for the stochastic and the chiral model of [17, 20], respectively; for the resulting analytic expression we refer to those papers. The class for which this is the case is that of *isotropic* models, i.e. with equal densities of left and right mirrors. The elements (3.8) of the diffusion tensor are then equal: $D_+ = D_- = D$. According to (4.2) we have $\lambda_1 = \lambda_2$, and we conclude from (A2.11) that the additional term in the denominator vanishes, leaving the denominator symmetric for $x \leftrightarrow -x$, causing the (antisymmetric) term with C_ℓ in the numerator to vanish in the integration, and we recover the integral we calculated analytically in [17]. However, this does not imply that the results will be the same as for the stochastic model (where we always have $\gamma^L = \gamma^R$), or the chiral model of [20] with $\gamma^L = \gamma^R$, because the collision operators entering in the EMA condition (6.2) are different from the T^L and T^R in the other models. The fact that we have an analytical result for the ring integral, together with quadratic EMA equations for the eigenvalues, makes the calculation quite feasible.

The most obvious isotropic model is that with $\beta = 0$ and $\gamma^L = \gamma^R = \frac{1}{2}c$ for c from 0 to 1 (full lattice). The results from the present kinetic theory method are displayed in figure 4. It shows that all ring approximations and the EMA are below the Boltzmann values; the EMA remains below Boltzmann for $c = 1$, while the ring and repeated-ring approximations bend back to the Boltzmann value as the full lattice is approached.

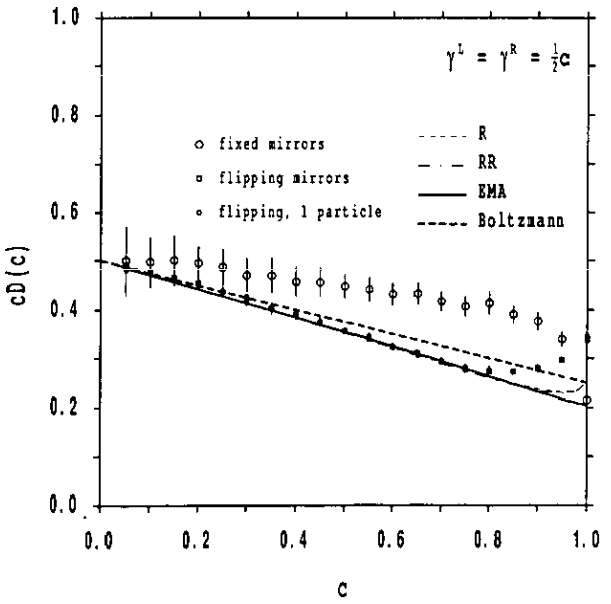

Figure 4. Mirror model for $\beta = 0$ and $\gamma^L = \gamma^R = \frac{1}{2}c$. Simulations from [23].

For this model we also performed computer simulations, which agree within error bars with the much more extensive computer simulations performed by Kong and Cohen [23]; the latter are displayed in figure 4. These simulations confirm the existence of a *positive* deviation from the Boltzmann diffusion coefficient at intermediate densities [23]. This effect was only vaguely observable in the early simulations [22]. The positive

deviation is peculiar, because usually ring collisions, as they refer to returns to the same site, with on the average a velocity $v_x(t)$ opposite to $v_x(0)$, yield a negative contribution to the VACF and the diffusion coefficient. Usually, for low densities the ring collisions are the first correction to the Boltzmann value. The stochastic model of [17] fits this picture. The remarkable positive deviation in the mirror model is explained in [23] in a qualitative manner as to originate from local fluctuations in the densities of mirrors: an excess of one type induces staircase-like behaviour over the region of the fluctuation. It is similar to the rattling behaviour between two nearby trees in the Ehrenfest wind–tree model [33]. It is further argued that this effect is responsible for the mere existence of diffusion in this model. Note the peculiarity that for the full lattice, the simulation result lies *below* the Boltzmann value.

The fluctuations of the densities of left and right mirrors are assumed to have much less effect in the case of the *flipping mirror* model: upon being hit by a moving particle, the mirror flips orientation. This introduces interactions between the moving particles, an effect that is definitely not accounted for by the present kinetic theory, see section 7. However, the main effect will be a randomization of the mirror orientation. In general, flipping of the mirrors causes the moving particle(s) to randomize the mirror orientations. Consequently, the geometrical constraint that a moving particle can only return twice to its point of origin, with only uncorrelated collisions in between, is lifted. The model with flipping mirrors also has much better ergodic properties: simulations seem to indicate that phase space consists essentially of a single orbit [22, 23].

Simulations of this model show a *negative* deviation from the Boltzmann value for c up to $c = 0.85$. In spite of the inapplicability of the present analysis for the fixed mirror model to the *flipping mirror model*, the EMA and the ring approximations seem to describe the simulation data quite well over a reasonable range of densities, as we show in figure 4. Note that here, only for the almost full lattice, the simulations exceed Boltzmann, contrary to what we observe for the fixed mirror case.

For the (fixed) mirror model with $\gamma^{\mathrm{L}} = \gamma^{\mathrm{R}} = \frac{1}{2}c$ the deviations from Boltzmann are most prominent at densities of $c = 0.5$–0.9. In order to investigate these peculiarities at intermediate densities, we study the model with tunable parameters, namely flipping and transmission probabilities. In section 7 we introduced these models and discussed them by considering typical trajectories that may be responsible for the effects at low probabilities. The collision sequences of figure 3 are so-called 'orbiting' trajectories. Our kinetic theory (including the application to flipping mirrors in section 7) does not account for them, as it only includes (the whole set of) ring and nested-ring diagrams [18]. In figure 5 we present the simulation results for the mirror model with *transmission* probability. In order to have a constant Boltzmann value we kept $c^* \equiv c(1 - p_{\mathrm{tr}})$ fixed; then $D_{BA} = (2c^*)^{-1} - \frac{1}{4}$. We indeed observe a phase transition for $p_{\mathrm{tr}} = 0$. Moreover, the deviation from Boltzmann seems just to *change sign* with respect to the fixed mirror case; the density considered is $c = 0.7$. For other densities the competition between the different contributions, see figure 3, may give different results. In figure 6 we plot the simulations for the *flipping* mirror model as a function of the flip probability p_{fl}. In figure 6(a) there is only one moving particle present in the system. Here we find the same features, only less prominent. This difference between these two models is in line with our low-probability remarks in section 7 that for the flipping mirror model the effect is caused by the more complicated, and thus less probable trajectories of figure 3(c), while for the transmission model the orbits of figure 3(b) are important. Finally, in figure 6(b), we present the data for the flipping mirror model with many particles (typically 1500 in a 500×500 lattice). Here,

the interactions clearly randomize the dynamics, and we find Boltzmann diffusion coefficients already for small flipping probabilities [21]. This reflects the fundamental difference between the model with a single moving particle and the one with many particles, which could not clearly be concluded from the results at $p_{\rm fl} = 1$, see figure 4. We have also run simulations for other densities, i.e. $c = 0.4, 0.5, 0.6, 0.8, 0.9, 0.95$ and 1.00. The features for $c < 1.0$ and small flipping probabilities are qualitatively the same. It may be that for high flipping probability, entirely different effects play a role [25]. We note that the moving particle needs to 'see' that there is a transmission or flipping probability. In order to obtain the full effect, we performed the $p_{\rm fl} = 0.01$ and $p_{\rm tr} = 0.01$ simulations for t up to 3000 units, instead of $t = 1000$. In order to make the error bars of the $p = 0$ and $p = 1$ data visible, we plotted the data a little inside the frame.

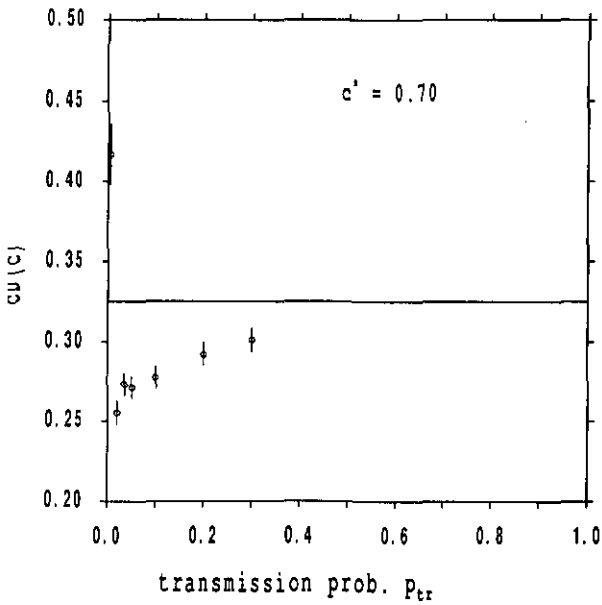

Figure 5. Results for mirrors with transmission probability, at mirror density $c^* = 0.7$.

We continue with a brief discussion of (fixed-mirror) models with reflector sites as well as mirror sites. Here, $\beta \neq 0$, but still $\gamma^{\rm L} = \gamma^{\rm R}$. So these models are isotropic and thus involve ring integrals that can be calculated analytically. Preliminary results calculated in effective medium approximation (EMA) indicate that the diffusion coefficient practically vanishes as soon as the scatterer density is non-zero. This corresponds to the notion that there is no diffusion in this case, as the average length of the trajectory is proportional to β^{-1} and the particle simply moves up and down between the endpoints, which contain reflectors. The probability for the particle to traverse the lattice (of linear size $L \sim 1000$) without being trapped in such an orbit, is thus of the order of $\exp(-\beta L)$. Although the simulations were unable to confirm or exclude whether diffusion does exist at large times in the chiral and in the mirror model, here the reflectors destroy *any* behaviour that remotely looks like diffusion. It is surprising that even in this extreme case the EMA is capable of explaining the absence of diffusion in the presence of reflectors, at least in a qualitative sense. For

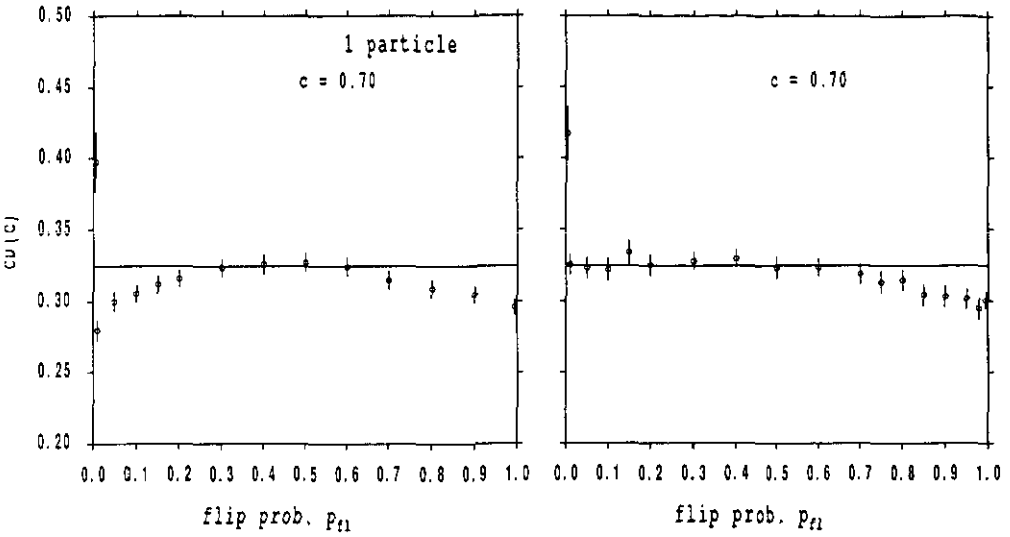

Figure 6. Results for mirrors with flipping probability, at mirror density $c = 0.7$: (*a*) 1 moving particle; (*b*) many moving particles, interacting through mirrors.

this case the breakdown of the Boltzmann equation is obvious. A short-time simulation with parameter values $\beta = 0.1c$, $\gamma^{\mathrm{L}} = 0.45c$ and $\gamma^{\mathrm{R}} = 0.45c$ yields diffusion coefficients of the order of 0.1 and 0.02 for c values of 0.1 and 0.2, respectively, which is indeed practically zero. We used only 200 time steps. It is not expected that this qualitative feature depends on whether we have an isotropic model ($\gamma^{\mathrm{L}} = \gamma^{\mathrm{R}}$) or an anisotropic model ($\gamma^{\mathrm{L}} \neq \gamma^{\mathrm{R}}$).

For the general *anisotropic* case, i.e. fixed mirrors with $\gamma^{\mathrm{L}} \neq \gamma^{\mathrm{R}}$ and no restrictions on β, the ring integral has the general form (A2.9), which we evaluated numerically. However, while in the cases described before the iteration of the EMA equations converged sufficiently rapidly, we did not obtain convergence for any deviation from isotropy. Numerical methods do not yield solutions, indicating that the effective medium approximation does not work out well for this model. The same is the case for the *self-consistent* ring and repeated-ring approximations (SRA and SRRA). See also [18] for similar technical difficulties. Of course, it is possible to calculate the Boltzmann approximation and the ring and repeated-ring approximation (RA and RRA), as they are straightforward calculations. The results for the case $\gamma^{\mathrm{L}} = \frac{2}{5}c$, $\gamma^{\mathrm{R}} = \frac{3}{5}c$ are displayed in figure 7, together with simulation data. Our simulations were carried out with lattices of up to 1000×1000 sites and periodic boundary conditions. They exhibit qualitatively the same behaviour as the isotropic case, for both elements of the (diagonalized) diffusion tensor. We observe that the data for the larger of the two elements lie farther away from the Boltzmann prediction than those for the lower. This is consistent with our earlier remarks (section 4) concerning the model with *only one type* of mirrors. One element of the diffusion tensor, corresponding to diffusion in the diagonal direction, diverges because the particle has a uniform velocity parallel, say, to the right mirrors, in the (1,1) direction, and the mean square displacement $\langle (n_x + n_y)^2 \rangle$ grows as t^2. In the perpendicular (1, 1) direction, the mean square displacement $\langle (n_x - n_y)^2 \rangle \simeq 2Dt$ as $t \to \infty$ with D *exactly* given by the Boltzmann equation (4.3), because correlated collisions are absent in this model. We also see that it takes time for the particles to explore the deviations from Boltzmann; this is seen

most clearly by the difference in the $t = 200$ data and the $t = 2000$ data for the partial diffusion coefficient D_+.

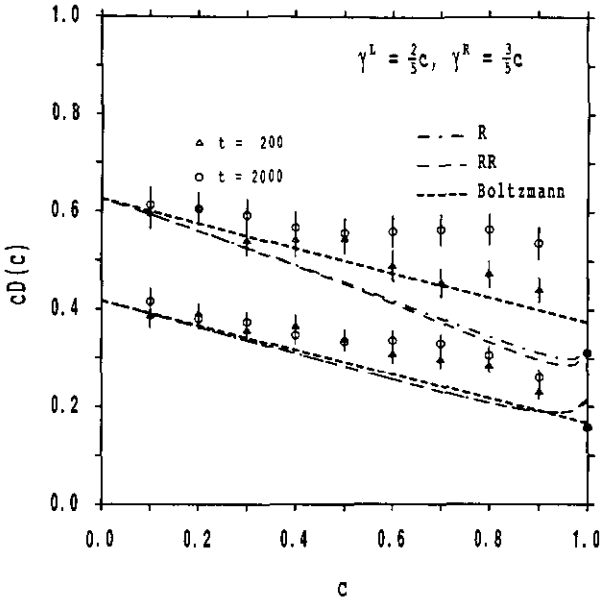

Figure 7. Anisotropic mirror model with $\gamma^L = \frac{2}{5}c$, $\gamma^R = \frac{3}{5}c$. Simulation results for D at several values of time t.

An interesting property of the fixed mirror model without reflectors is that diffusion still exists at high densities. This has been shown for a completely filled lattice with $\gamma^L = \gamma^R = \frac{1}{2}$ by mapping it on two-dimensional bond percolation [34]. It is also possible to calculate the asymptotic long-time form of the probability distribution for displacements. It turns out that the second moment of this distribution grows linearly with time, allowing the definition of a diffusion coefficient by using the Einstein relation. On the other hand, higher moments no longer show Gaussian behaviour, implying that the probability distribution does not satisfy Fick's diffusion equation. Although very slowly, the kurtosis, defined as $K = (\langle x^4 \rangle - 3\langle x^2 \rangle^2)/\langle x^2 \rangle^2$, grows with time. In the Gaussian case the kurtosis goes to zero for long times. Kong and Cohen [25] have performed extensive computer simulations of the mirror model, and analysed the anomalous diffusion of the model in great detail. They find that for the isotropic model ($\gamma^L = \gamma^R = \frac{1}{2}c$) the kurtosis increases from zero at low densities to values of 1.27±0.16, 1.66±0.13 and 3.6±0.2 for c values of 0.9, 0.95 and 1.0, respectively. The simulations were run for 4000 mean free times $t_{mf} \sim c^{-1}$. Kinetic theory methods, able to explain this peculiar behaviour, are not available.

In summary we make the following points.

(i) We have seen that the present kinetic theory (ring approximations and EMA), and also the molecular chaos assumption of the Boltzmann equation, are unable to explain the intriguing results for the mirror model with *fixed* mirrors.

(ii) The present kinetic theory analysis for the *flipping* mirror model yields no deviations from the Boltzmann diffusion coefficient, neither in the repeated-ring approximation nor in the full EMA. This does not agree with the simulation data.

(iii) Unexpectedly, however, our EMA results for *fixed* mirrors seem to describe the

simulation data for the *flipping* mirrors of [23] quite well over a large range of densities ($c \leq 0.9$).

(iv) Our study of small flipping and transmission probabilities provides arguments that the deviations of kinetic theory from the simulations are caused by orbiting collision sequences. (See [17, 18, 20] and figure 3.) They are more important in deterministic than in stochastic models. Unfortunately, they are not accounted for in the kinetic theory. It would be of interest to analyse theoretically the contributions from the orbiting collision sequences.

(v) In general, flipping and transmission probability have a randomizing effect, yielding Boltzmann diffusion coefficients. However, although this is indeed the case for *intermediate* flipping or transmission probabilities ($p_{\rm fl}, p_{\rm tr} = 0.4 - 0.6$), it is definitely *not* true for *small* transmission probabilities or *small* flipping probabilities in the case of one moving particle.

(vi) For the fixed mirror model without reflectors diffusion still exists at high densities [34]. The second moment of the probability distribution grows linearly with time, allowing the definition of a diffusion coefficient by using the Einstein relation.

(vii) On the other hand, higher moments no longer show Gaussian behaviour, implying that the probability distribution does not satisfy Fick's diffusion equation. Also this is an area for which further theoretical investigations would be of interest.

Acknowledgments

The author would like to thank E G D Cohen and X P Kong for interesting discussions, and for the use of their simulation data. He also thanks H van Beijeren, M H Ernst, B Nienhuis, Th W Ruijgrok and J A Tjon for comments, suggestions and discussions. The work of the author is financially supported by the Stichting voor Fundamenteel Onderzoek der Materie (FOM), which is sponsored by NWO.

Appendix 1. Green–Kubo formula for partial diffusion

This appendix sketches the derivation of the Green–Kubo formula for the 'partial' diffusion coefficients, as introduced at the end of section 2. Writing the mean square displacement for two dimensions as

$$\langle n_x^2 + n_y^2 \rangle = \tfrac{1}{2}\langle (n_x + n_y)^2 + (n_x - n_y)^2 \rangle \tag{A1.1}$$

we define the (time-dependent) partial diffusion coefficients $D_+(t)$ and $D_-(t)$ by

$$4D_\pm(t) \equiv \Delta_t \langle (n_x(t) \pm n_y(t))^2 \rangle. \tag{A1.2}$$

Recall that for the isotropic case we have $2D = \Delta_t \langle n_x^2 \rangle$. Applying the time difference and using the fact that

$$n_\alpha(t+1) = \sum_{\tau=0}^{t} v_\alpha(\tau) \tag{A1.3}$$

we can write this as the average of:

$$v_x(t)\left(n_x(t+1)+n_x(t)\right)+v_y(t)\left(n_y(t+1)+n_y(t)\right)$$
$$+2\sum_{\sigma,\tau=0}^{t} v_x(\sigma)v_y(\tau)-2\sum_{\sigma,\tau=0}^{t-1} v_x(\sigma)v_y(\tau). \tag{A1.4}$$

After some more algebra, this can be written as

$$\left\langle 2\sum_{\tau=0}^{t}\left(v_x(t)+v_y(t)\right)\left(v_x(\tau)+v_y(\tau)\right)\right\rangle-\langle v_x^2(t)\rangle-\langle v_y^2(t)\rangle. \tag{A1.5}$$

For D_- the derivation is similar. Finally we have, using time reversal symmetry and $\langle v_x^2(o)\rangle=\frac{1}{2}$ (in two dimensions):

$$D_{\pm}=\frac{1}{2}\sum_{\tau=0}^{t}\langle v_{\pm}(\tau)v_{\pm}(0)\rangle-\tfrac{1}{4} \tag{A1.6}$$

where

$$v_{\pm}(t)\equiv v_x(t)\pm v_y(t). \tag{A1.7}$$

With these definitions of D_+ and D_- the total diffusion coefficient is then found to be

$$D\equiv\tfrac{1}{2}\left(D_++D_-\right)=\frac{1}{2}\sum_{t=0}^{\infty}[\langle v_x(t)v_x(0)\rangle+\langle v_y(t)v_y(0)\rangle]-\tfrac{1}{4} \tag{A1.8}$$

just as it should be. Used here is that $\langle v_x(t)v_y(0)\rangle=0$, etc.

Appendix 2. Ring integral

For the calculation of the transition probabilities, (i.e. the effective densities of the different scatterers) in the various approximations, we restrict ourselves to the $z=0$ case, as we aim for the static diffusion coefficient. We evaluate the eigenvalues of the ring operator

$$R(z=0)=\int_q\left(\mathrm{e}^{\mathrm{i}qV}-1-K'(z=0)\right)^{-1}. \tag{A2.1}$$

They are:

$$r_\ell=\langle\psi_\ell|R|\psi_\ell\rangle=\int_q\langle\psi_\ell|A_\ell\rangle \tag{A2.2}$$

with A_ℓ satisfying

$$\left(\mathrm{e}^{\mathrm{i}qV}-1-cT^{\mathrm{e}}\right)|A_\ell\rangle=|\psi_\ell\rangle \tag{A2.3}$$

The matrix elements $B_{\ell\ell'}$ are defined as [17]

$$B_{\ell'\ell} = \langle\psi_{\ell'}|(e^{iqV} - 1)^{-1}|\psi_\ell\rangle. \tag{A2.4}$$

The effective collision matrix $-cT^e = \Lambda$ is decomposed into projection operators P_ℓ on the eigenspaces (3.3) of the reflection symmetric operator:

$$-cT^e = \Lambda = \lambda_1 P_1 + \lambda_2 P_2 + \lambda_3 P_3 \tag{A2.5}$$

where

$$P_\ell = |\psi_\ell\rangle\langle\psi_\ell|. \tag{A2.6}$$

The values or expressions to be substituted for the λ will correspond to the actual approximation (RA, RRA, SRA, SRRA or EMA) that we wish to study. The equations for the components of the vector A_ℓ are formally the same as for the chiral model that we studied in [20]:

$$\begin{pmatrix} 1+\lambda_1 B_{11} & \lambda_2 B_{12} & \lambda_3 B_{13} \\ \lambda_1 B_{21} & 1+\lambda_2 B_{22} & \lambda_3 B_{23} \\ \lambda_1 B_{31} & \lambda_2 B_{32} & 1+\lambda_3 B_{33} \end{pmatrix} \begin{pmatrix} \langle\psi_1|A_\ell\rangle \\ \langle\psi_2|A_\ell\rangle \\ \langle\psi_3|A_\ell\rangle \end{pmatrix} = \begin{pmatrix} B_{1\ell} \\ B_{2\ell} \\ B_{3\ell} \end{pmatrix}. \tag{A2.7}$$

We find for the matrix elements $B_{\ell'\ell}$:

$$\begin{aligned} B_{11} &= B_{22} = B_{33} = -\tfrac{1}{2} & \qquad B_{12} &= B_{21} = 0 \\ B_{13} &= B_{31} = -ih_x + ih_y & \qquad B_{23} &= B_{32} = -ih_x - ih_y \end{aligned} \tag{A2.8}$$

with $h_\alpha \equiv \frac{1}{4}\sin q_\alpha/(1-\cos q_\alpha)$. The $\langle\psi_{\ell'}|A_\ell\rangle$ can now be calculated. However, after carrying out the algebra one concludes that, for this model, the ring integral cannot be written in the familiar form that one finds for the stochastic model of [17] or the chiral model of [20]. The cross terms, i.e. some $\sin q_\alpha$ terms, do not drop out. The result is:

$$r_\ell = \int_q \frac{A_\ell + 16B_\ell(h_x^2 + h_y^2) + 16C_\ell h_x h_y}{E + 16F(h_x^2 + h_y^2) + 16Gh_x h_y} \tag{A2.9}$$

for $\ell = 1, 2, 3$. The coefficients A_ℓ, B_ℓ, E and F are given by:

$$\begin{aligned} A_1 &= -\tfrac{1}{2}(1-\tfrac{1}{2}\lambda_2)(1-\tfrac{1}{2}\lambda_3) & \qquad B_1 &= \tfrac{1}{16}\lambda_3(1-\lambda_2) \\ A_2 &= -\tfrac{1}{2}(1-\tfrac{1}{2}\lambda_1)(1-\tfrac{1}{2}\lambda_3) & \qquad B_2 &= \tfrac{1}{16}\lambda_3(1-\lambda_1) \\ A_3 &= -\tfrac{1}{2}(1-\tfrac{1}{2}\lambda_1)(1-\tfrac{1}{2}\lambda_2) & \qquad B_3 &= \tfrac{1}{16}(\lambda_1+\lambda_2-\lambda_1\lambda_2) \\ E &= (1-\tfrac{1}{2}\lambda_1)(1-\tfrac{1}{2}\lambda_2)(1-\tfrac{1}{2}\lambda_3) & \qquad F &= \tfrac{1}{16}\lambda_3(\lambda_1+\lambda_2-\lambda_1\lambda_2). \end{aligned} \tag{A2.10}$$

which are the same as in [20], but now there is also

$$C_1 = -\tfrac{1}{8}\lambda_3 \qquad C_2 = \tfrac{1}{8}\lambda_3 \qquad C_3 = \tfrac{1}{8}(\lambda_1 - \lambda_3) \qquad G = \tfrac{1}{8}\lambda_3(\lambda_2 - \lambda_1). \tag{A2.11}$$

Because of these extra terms (especially in the denominator), the ring integral is different from the one we calculated analytically in [17]. Therefore the integral was evaluated numerically.

References

[1] Wolfram S 1986 *J. Stat. Phys.* **45** 471; 1984 *Nature* **311** 419

[2] Frisch U, d'Humieres D, Hasslacher N, Lallemand P, Pomeau Y and Rivet J P 1987 *Complex Systems* **1** 649
Henon M 1987 *Complex Systems* **1** 763
Rivet J P 1987 *Complex Systems* **1** 839

[3] Doolen G D, Frisch U, Hasslacher H, Orszag S and Wolfram (eds) 1987 *Lattice Gas Methods for Partial Differential Equations* (New York: Addison-Wesley)

[4] Doolen G D (ed) *Proc. Workshop on Lattice Gas Methods for PDE's, Los Alamos, September 1989* (New York: Addison-Wesley)

[5] Kadanoff L, McNamara G and Zanetti G 1987 *Complex Systems* **1** 791; 1989 *Phys. Rev.* A **40** 4527

[6] Monaco R (ed) 1988 *Proc. Workshop on Discrete Kinetic Theory, Lattice Gas Dynamics and Foundations of Hydrodynamics, Turin* (Singapore: World Scientific)

[7] Hauge E H 1974 *Transport Phenomena (Lecture Notes in Physics 31)* ed G Kirczenow and J Marro (Berlin: Springer) p 338

[8] Hauge E H and Cohen E G D 1969 *J. Math. Phys.* **10** 397

[9] Jepsen D W 1965 *J. Math. Phys.* **6** 405

[10] Lebowitz J L and Percus J K 1967 *Phys. Rev.* **155** 122; Lebowitz J L, Percus J K and Sykes J K 1968 *Phys. Rev.* **171** 224

[11] van Beijeren H 1982 *Rev. Mod. Phys.* **54** 195; van Beijeren H and Spohn H 1983 *J. Stat. Phys.* **31** 231

[12] McLennan J A 1989 *Statistical Mechanics* (New York: Prentice Hall)

[13] Dorfman J R and van Beijeren H 1977 *Statistical Mechanics, Part B: Time dependent processes* ed B J Berne (New York: Plenum) p 65

[14] van Leeuwen J M J and Weyland A 1967 *Physica* **36A** 457
Weyland A and van Leeuwen J M J 1968 *Physica* **38A** 35

[15] Ernst M H, van Velzen G A and Binder P M 1989 *Phys. Rev.* A **39** 4327

[16] van Velzen G A and Ernst M H 1988 *Proc. Workshop on Discrete Kinetic Theory, Lattice Gas Dynamics and Foundations of Hydrodynamics, Turin* (Singapore: World Scientific)

[17] Ernst M H and van Velzen G A 1989 *J. Phys. A: Math. Gen.* **22** 4611–32

[18] van Velzen G A 1990 *J. Phys. A: Math. Gen.* **23** 4953–76

[19] Gunn J M F and Ortuño M 1985 *J. Phys. A: Math. Gen.* **18** L1095

[20] van Velzen G A 1991 *J. Phys. A: Math. Gen.* 787–806

[21] Cohen E G D private communication

[22] Ruijgrok Th W and Cohen E G D 1988 *Phys. Lett.* **133A** 415

[23] Kong X P and Cohen E G D 1989 *Phys. Rev.* B **40** 4838

[24] Kong X P and Cohen E G D 1989 *Proc. Workshop on Lattice Gas Methods for PDE's* ed G D Doolen (New York: Addison-Wesley)

[25] Kong X P and Cohen E G D 1990 *Physica* D submitted

[26] van Velzen G A 1990 *PhD thesis* University of Utrecht

[27] Denteneer P and Ernst M H 1983 *J. Phys. C: Solid State Phys.* **16** L961; 1984 *Phys. Rev.* B **29** 1755

[28] Nieuwenhuizen Th M, van Velthoven P F J and Ernst M H 1986 *Phys. Rev. Lett.* **57** 2477; 1987 *J. Phys. A: Math. Gen.* **20** 4001

[29] Ernst M H, van Velthoven P F J and Nieuwenhuizen Th M 1987 *J. Phys. A: Math. Gen.* **20** 949; 1986 *J. Stat. Phys.* **45** 1001

[30] Ernst M H 1987 *J. Stat. Phys.* **48** 645

[31] van Velzen G A and Ernst M H 1987 *J. Stat. Phys.* **48** 677

[32] Grassberger P 1986 *J. Phys. A: Math. Gen.* **19** 2675

[33] Abraham D B and Gates D J 1974 *Physica* **72** 73

[34] Nienhuis B private communication

[35] van Kampen N G 1981 *Stochastic Processes in Physics and Chemistry* (Amsterdam: North-Holland)

[36] Kirkpatrick S 1973 *Rev. Mod. Phys.* **45** 574

[37] Webman I 1981 *Phys. Rev.* **47** 1496